Differential WW production in NNLO QCD

Stefan Kallweit

based on work with: T. Gehrmann[a], M. Grazzini[ab], P. Maierhöfer[a], A. v. Manteuffel[a], S. Pozzorini[ab], D. Rathlev[ab], L. Tancredi[a], M. Wiesemann[b]

[b] JHEP 1608 (2016) 140 [arXiv:1605.02716 [hep-ph]]
[a] Phys.Rev.Lett. 113 (2014) 21, 212001 [arXiv:1408.5243 [hep-ph]]

Rencontres de Moriond LII: QCD and High Energy Interactions
La Thuile, March 25–April 1, 2017

Outline

1. Motivation for NNLO QCD accuracy in VV production
2. Calculation of NNLO QCD cross sections in the MATRIX framework
3. Numerical MATRIX results for $\mathrm{pp}\,(\to \mathrm{W}^+\mathrm{W}^-) \to 2\ell 2\nu + \mathrm{X}$
   - Results for inclusive WW production at 13 TeV
   - Results for WW signal cuts in $2\ell 2\nu$ channel at 13 TeV
4. Corrections to WW production beyond NNLO QCD
5. Conclusions & Outlook

Data–theory comparison for VV cross sections — status winter 2017

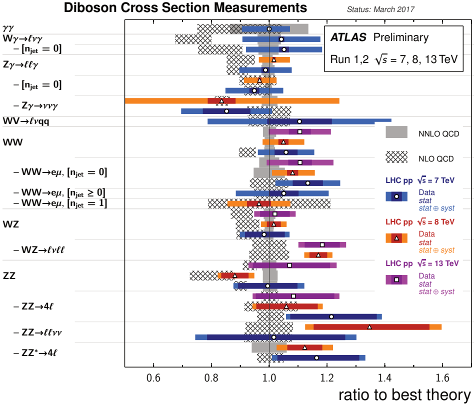

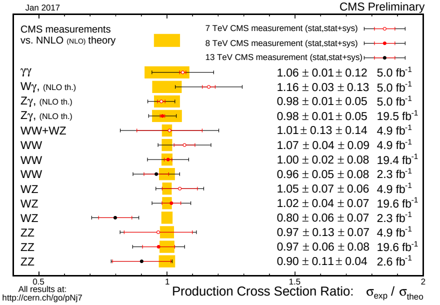

[CMS collaboration, January 2017]

[ATLAS collaboration, March 2017]

VV production (with leptonic decays) at NNLO QCD is important:

- Standard Model test → trilinear gauge-boson couplings
- Background for Higgs analyses and BSM searches

↪ **Inclusion of NNLO QCD corrections improves agreement with Standard Model.**

The MATRIX framework for automated NNLO+NNLL calculations

[Grazzini, SK, Rathlev, Wiesemann]

Amplitudes

OPENLOOPS (**COLLIER**, **CUTTOols**, ...)	**Dedicated 2-loop codes** (**VVAMP**, **GINAC**, **TDHPL**, ...)

MUNICH

MUlti-chaNnel Integrator at Swiss (CH) precision

q_{T} **subtraction** $\Leftrightarrow$ q_{T} **resummation**

NNLO → | NNLL →

MATRIX

MUNICH Automates qT subtraction and Resummation to Integrate X-sections.

Inclusive WW cross sections for relevant LHC energies

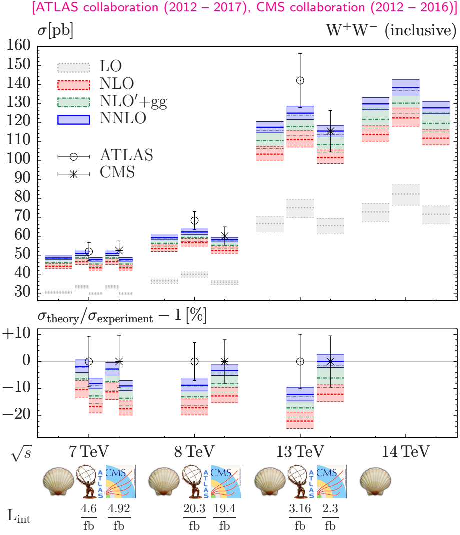

- MATRIX results with NNPDF3.0 PDF sets.

- **on-shell** (left): $m_{\ell\nu} = m_W$
  ATLAS (center): 8, 13, 14 TeV: $H \to WW^*$ included
  CMS (right): 8, 13, 14 TeV: $H \to WW^*$ not included
  ATLAS and **CMS**: 7 TeV: Predictions shown with (left) and without (right) $H \to WW^*$

- NLO/LO ranges from 44% to 56% (7 TeV to 14 TeV).

- NNLO/NLO ranges from 10% to 14% (7 TeV to 14 TeV).

- NNLO scale variation $\approx \pm 3\%$.
  $$\begin{pmatrix} M_W/2 \le \mu_R, \mu_F \le 2M_W \\ 1/2 \le \mu_R/\mu_F \le 2 \end{pmatrix}$$

- Loop-induced gg channel makes for about 35% of NNLO effect.

Inclusive distributions for reconstructed W's: p_{T,W_1}, p_{T,W_2}, m_{WW}

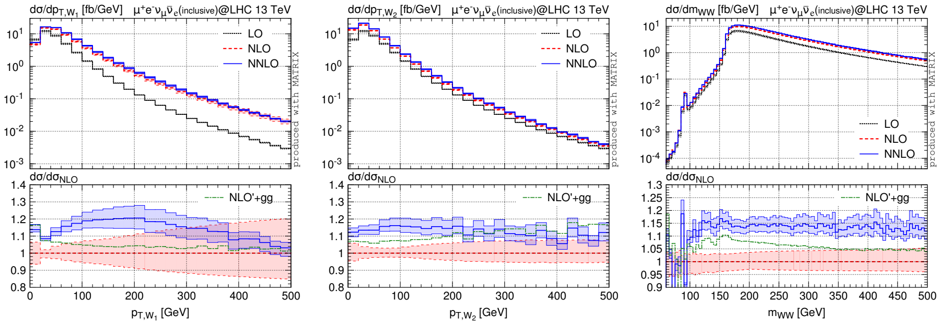

p_{T,W_1} and p_{T,W_2}:

- Giant NLO K-factor in p_{T,W_1}, but not in p_{T,W_2} (jet-recoil topologies).

m_{WW}:

- Threshold behaviour at $2\,m_W$.
- $Z \to 2\ell 2\nu$ peak well resolved.

- NLO and NNLO scale-variation bands typically do not overlap.
  - ↪ New channels open up at NNLO (loop-induced gg channel, but also e.g. qq).
- NLO$'$ + gg provides only about 35% of the NNLO corrections.
  - ↪ No sufficient approximation of full NNLO result (both normalization and shape).

Definition of top-contamination free WW cross section

- Straightforward in 4FNS (massive b's $\to$ $WWb\bar{b}$ finite and can be split off)
- Non-trivial in 5FNS (massless b's $\to$ WW and $WWb\bar{b}$ connected by IR structure)
  - Single-top production enters at NLO.
  - Top-pair production enters at NNLO.

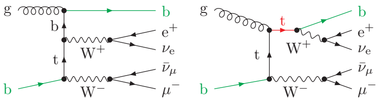

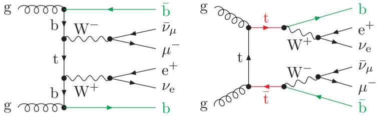

$\hookrightarrow$ Huge "higher-order corrections" result from top-resonance contamination in 5FNS (cross-section enhancement of 30%/400% at NLO/NNLO for $\sqrt{s} = 8$ TeV).

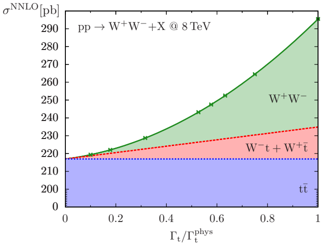

- Γ_t-dependence of NNLO cross section can be used to isolate the different processes:

  $\sigma_{WW} \propto 1, \quad \sigma_{tW} \propto 1/\Gamma_t, \quad \sigma_{t\bar{t}} \propto 1/\Gamma_t^2.$

- Parabolic fit of $(\Gamma_t/\Gamma_t^{\text{phys}})^2$-rescaled NNLO cross section delivers σ_{WW}, σ_{tW}, $\sigma_{t\bar{t}}$.

$\hookrightarrow$ $\approx$ 1-2% agreement between 4FNS and 5FNS.

Fiducial off-shell cross sections for $\mathrm{pp}\,(\to \mathrm{W^+W^-}) \to 2\ell 2\nu + \mathrm{X}$

Setup motivated by the ATLAS analysis @ 8 TeV [ATLAS collaboration (2014 & 2016)]

	$\sigma_{\mathrm{fiducial}}(W^+W^-\text{-cuts})$ [fb]		$\sigma/\sigma_{\mathrm{NLO}} - 1$	
$\sqrt{s}$	8 TeV	13 TeV	8 TeV	13 TeV
LO	$147.23\ (2)\,^{+3.4\%}_{-4.4\%}$	$233.04(2)\,^{+6.6\%}_{-7.6\%}$	-3.8%	$-\ 1.3\%$
NLO	$153.07\ (2)\,^{+1.9\%}_{-1.6\%}$	$236.19(2)\,^{+2.8\%}_{-2.4\%}$	0	0
NLO′	$156.71\ (3)\,^{+1.8\%}_{-1.4\%}$	$243.82(4)\,^{+2.6\%}_{-2.2\%}$	$+2.4\%$	$+\ 3.2\%$
NLO′$+gg$	$166.41\ (3)\,^{+1.3\%}_{-1.3\%}$	$267.31(4)\,^{+1.5\%}_{-2.1\%}$	$+8.7\%$	$+13.2\%$
NNLO	$164.16(13)\,^{+1.3\%}_{-0.8\%}$	$261.5(2)\,^{+1.9\%}_{-1.2\%}$	$+7.2\%$	$+10.7\%$

- Results refer to only one different-flavour channel: $\mathbf{pp \to e^- \mu^+ \nu_\mu \bar{\nu}_e + X}$
- Event selection imposes a **jet veto**.
  - ↪ Usual scale variation underestimates missing higher-order corrections.
- NLO corrections amount to about $+4\%$ $(+1\%)$ wrt. LO result at 8 (13) TeV.
- NNLO corrections amount to about $+7\%$ $(+10\%)$ wrt. NLO result at 8 (13) TeV.
- The positive impact of the NNLO corrections is entirely due to the loop-induced gg contribution, which is about $+6\%$ $(+10\%)$ wrt. NLO result at 8 (13) TeV.
  - ↪ $\mathcal{O}(\alpha_s^2)$ corrections to $q\bar{q}$ are negative and amount to roughly -2% (-3%).

Distributions with WW signal cuts: p_{T,l_1}, p_{T,l_2}, $p_{T,\mathrm{miss}}$

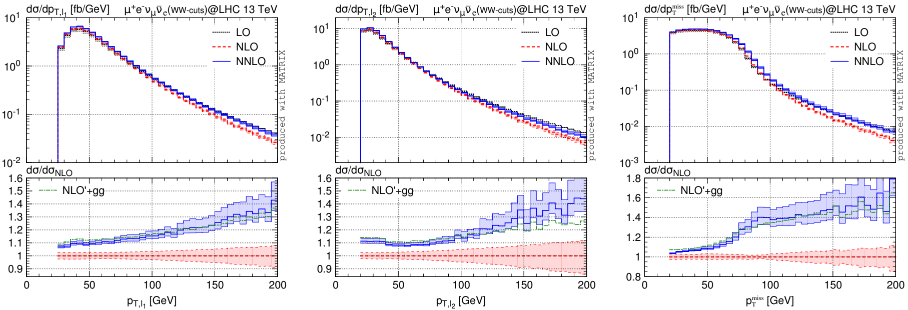

- The loop-induced gg contribution dominates the NNLO corrections.
  ↪ NLO and NNLO scale-variation bands typically do not overlap.
  (gg channel not covered by scale-variation uncertainties from $q\bar{q}$ channel)
- By and large NLO$'$ + gg approximates the full NNLO prediction very well (in particular for observables without strong kinematical constraints).
- However, shape distortions of up to about 10% result from genuine NNLO corrections (compared to NLO$'$ + gg approximation).

Di-lepton distributions with WW signal cuts: m_{ll}, $\Delta\phi_{ll}$, $\Delta\phi_{ll,\nu\nu}$

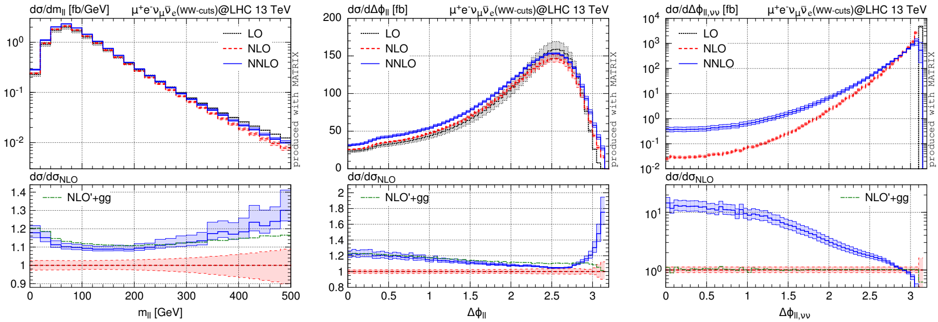

m_{ll} and $\Delta\phi_{ll}$ ($\ll \pi$):

- The loop-induced gg contribution dominates the NNLO corrections.
  - ↪ NLO and NNLO scale-variation bands typically do not overlap.
- Shape distortions of up to about 10% result from genuine NNLO corrections.

$\Delta\phi_{ll}$ ($\lesssim \pi$) and $\Delta\phi_{ll,\nu\nu}$:

- Phase-space regions that imply the presence of QCD radiation:
  - Huge NNLO corrections
  - Loop-induced gg contribution cannot approximate the shapes of full NNLO corrections.

Corrections to WW production beyond NNLO QCD

NLO QCD corrections to gg $\to \mathbf{W^+W^-}$ (gg-channel, massless 2-loop amplitudes)
[Caola, Melnikov, Röntsch, Tancredi (2015)]
(based on amplitudes from [Caola, Henn, Melnikov, Smirnov, Smirnov (2015); von Manteuffel, Tancredi (2015)])

- The LO gg-fusion cross section is increased by $\mathcal{O}(24\% - 80\%)$ for $M_\mathrm{W}/2 < \mu_\mathrm{R} = \mu_\mathrm{F} < 2M_\mathrm{W}$ at $\sqrt{s} = 8\,\mathrm{TeV}$ (slightly smaller at $\sqrt{s} = 13\,\mathrm{TeV}$).
  - ↪ Corresponds to increase of full NLO QCD prediction by about **+2%** at $\sqrt{s} = 8$ and $13\,\mathrm{TeV}$ (covered by the NNLO QCD scale-uncertainty estimate)
- In the ATLAS fiducial region, NLO QCD corrections to gg shrink to about $+20\%$.
- **NLO QCD to gg $\to \mathbf{W^+W^-}$** including interference effects with off-shell Higgs.
  [Caola, Dowling, Melnikov, Röntsch, Tancredi (2016)]

NLO EW corrections to off-shell $\mathbf{W^+W^-}$ production
[Biedermann, Billoni, Denner, Dittmaier, Hofer, Jäger, Salfelder (2016)]

- Corrections of about **−4% (−3%)** wrt. the inclusive (fiducial ATLAS) cross section at LO for both $\sqrt{s} = 8, 13\,\mathrm{TeV}$.
  - ↪ Larger (typically tens of per cent) corrections at high transverse momenta.
- Contribution from $\gamma\gamma$-induced process of about **+1%** wrt. both the inclusive and the fiducial ATLAS cross section at LO for both $\sqrt{s} = 8$ and $13\,\mathrm{TeV}$.

Conclusions & Outlook

MATRIX – an automated framework to perform fully differential NNLO (+NNLL) QCD computations for colourless final-state production – introduced, which is based on

- the **MUNICH** Monte Carlo integrator,
- the **q_T subtraction** (+resummation) method,
- **OPENLOOPS** and dedicated 2-loop amplitudes from **VVAMP**.

NNLO QCD predictions for
$\mathbf{pp\,(\to W^+W^-) \to 2\ell 2\nu + X}$

- **inclusive:** NNLO/NLO: **10%** to **14%** (7 TeV to 14 TeV) (≈ 35% from gg).
- **different situation with jet-veto:** *gg* dominates, $q\bar{q}$ slightly negative.

Future developments in MATRIX

- combination with NLO EW corrections
- NLO QCD corrections to gg channel
- **first public release . . .**

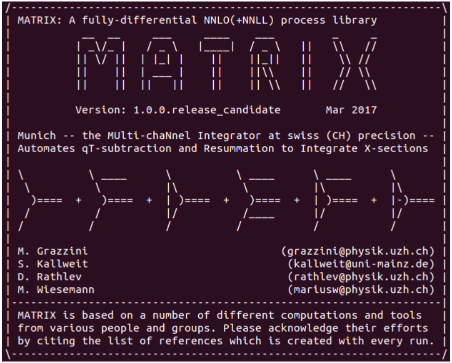

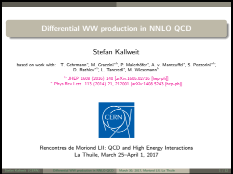

01

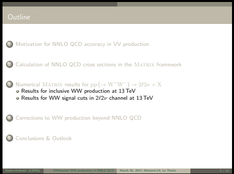

02

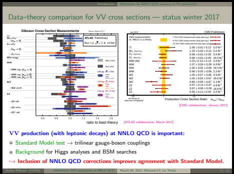

03

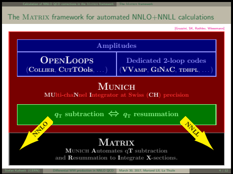

04

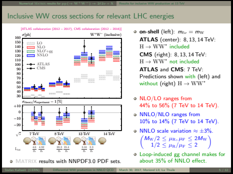

05

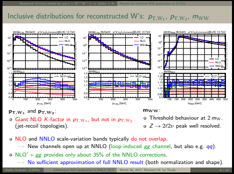

06

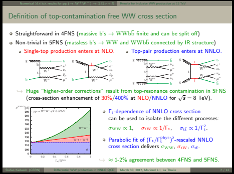

07

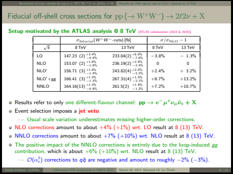

08

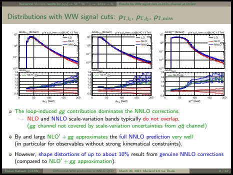

09

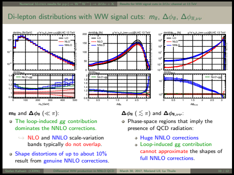

10

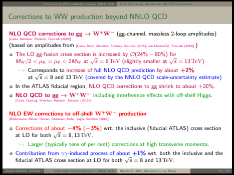

11

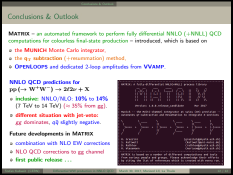

12

Backup

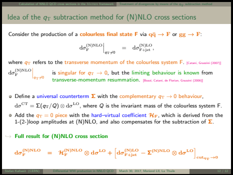

B01

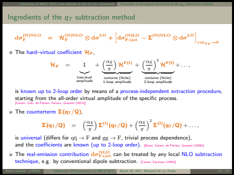

B02

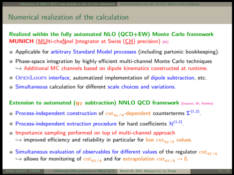

B03

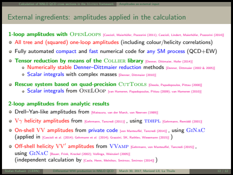

B04

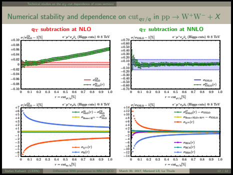

B05

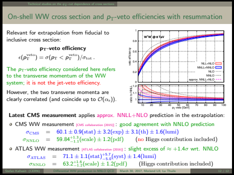

B06

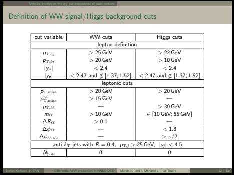

B07

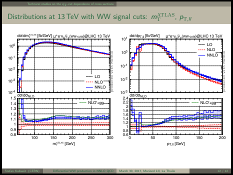

B08

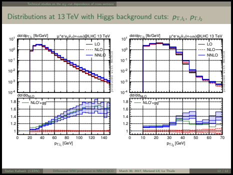

B09

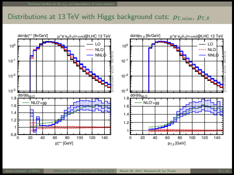

B10

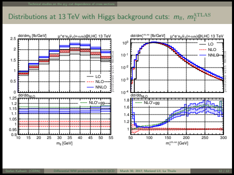

B11

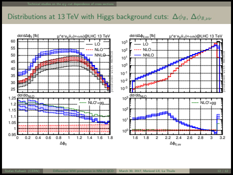

B12

Idea of the q_T subtraction method for (N)NLO cross sections

Consider the production of a **colourless final state F** via $\mathbf{q\bar{q} \to F}$ or $\mathbf{gg \to F}$:

$$\mathrm{d}\sigma_{\mathrm{F}}^{\mathrm{(N)NLO}}\Big|_{q_T \neq 0} = \mathrm{d}\sigma_{\mathrm{F+jet}}^{\mathrm{(N)LO}},$$

where q_T refers to the transverse momentum of the colourless system F. [Catani, Grazzini (2007)]

$\mathrm{d}\sigma_{\mathrm{F}}^{\mathrm{(N)NLO}}\Big|_{q_T \neq 0}$ is singular for $q_T \to 0$, but the limiting behaviour is known from transverse-momentum resummation. [Bozzi, Catani, de Florian, Grazzini (2006)]

- Define a universal counterterm $\mathbf{\Sigma}$ with the complementary $q_T \to 0$ behaviour, $\mathrm{d}\sigma^{\mathrm{CT}} = \Sigma(q_T/Q) \otimes \mathrm{d}\sigma^{\mathrm{LO}}$, where Q is the invariant mass of the colourless system F.
- Add the $q_T = 0$ piece with the hard–virtual coefficient $\mathcal{H}_{\mathrm{F}}$, which is derived from the 1-(2-)loop amplitudes at (N)NLO, and also compensates for the subtraction of $\mathbf{\Sigma}$.

↪ **Full result for (N)NLO cross section**

$$\mathrm{d}\sigma_{\mathrm{F}}^{\mathrm{(N)NLO}} = \mathcal{H}_{\mathrm{F}}^{\mathrm{(N)NLO}} \otimes \mathrm{d}\sigma^{\mathrm{LO}} + \left[\mathrm{d}\sigma_{\mathrm{F+jet}}^{\mathrm{(N)LO}} - \Sigma^{\mathrm{(N)NLO}} \otimes \mathrm{d}\sigma^{\mathrm{LO}}\right]_{\mathrm{cut}_{q_T} \to 0}$$

Ingredients of the q_T subtraction method

$$\mathbf{d\sigma_F^{(N)NLO} = \mathcal{H}_F^{(N)NLO} \otimes d\sigma^{LO} + \left[d\sigma_{F+jet}^{(N)LO} - \Sigma^{(N)NLO} \otimes d\sigma^{LO}\right]_{cut_{q_T}\to 0}}$$

- The hard–virtual coefficient $\mathcal{H}_F$,

$$\mathcal{H}_F = \underbrace{1}_{\substack{\text{tree-level}\\ \text{amplitude}}} + \underbrace{\left(\frac{\alpha_S}{\pi}\right)\mathcal{H}^{F(1)}}_{\substack{\text{contains (finite)}\\ \text{1-loop amplitude}}} + \underbrace{\left(\frac{\alpha_S}{\pi}\right)^2\mathcal{H}^{F(2)}}_{\substack{\text{contains (finite)}\\ \text{2-loop amplitude}}} + \ldots,$$

  is known up to 2-loop order by means of a process-independent extraction procedure, starting from the all-order virtual amplitude of the specific process.
  [Catani, Cieri, de Florian, Ferrera, Grazzini (2013)]

- The counterterm $\Sigma(q_T/Q)$,

$$\Sigma(q_T/Q) = \left(\frac{\alpha_S}{\pi}\right)\Sigma^{(1)}(q_T/Q) + \left(\frac{\alpha_S}{\pi}\right)^2\Sigma^{(2)}(q_T/Q) + \ldots,$$

  is universal (differs for $q\bar{q} \to F$ and $gg \to F$, trivial process dependence), and the coefficients are known (up to 2-loop order). [Bozzi, Catani, de Florian, Grazzini (2006)]

- The real-emission contribution $d\sigma_{F+jet}^{NLO}$ can be treated by any local NLO subtraction technique, e.g. by conventional dipole subtraction. [Catani, Seymour (1993)]

Numerical realization of the calculation

Realized within the fully automated NLO (QCD+EW) Monte Carlo framework
MUNICH (MUlti-chaNnel Integrator at Swiss (CH) precision) [SK]

- Applicable for arbitrary Standard Model processes (including partonic bookkeeping).
- Phase-space integration by highly efficient multi-channel Monte Carlo techniques
  ↪ Additional MC channels based on dipole kinematics constructed at runtime.
- OPENLOOPS interface, automatized implementation of dipole subtraction, etc.
- Simultaneous calculation for different scale choices and variations.

Extension to automated ($\mathbf{q_T}$ subtraction) NNLO QCD framework [Grazzini, SK, Rathlev]

- Process-independent construction of $\mathrm{cut}_{q_\mathrm{T}/q}$-dependent counterterms $\Sigma^{(1,2)}$.
- Process-independent extraction procedure for hard coefficients $\mathcal{H}^{(1,2)}$.
- Importance sampling performed on top of multi-channel approach
  ↪ improved efficiency and reliability in particular for low $\mathrm{cut}_{q_\mathrm{T}/q}$ values.
- Simultaneous evaluation of observables for different values of the regulator $\mathrm{cut}_{q_\mathrm{T}/q}$
  ↪ allows for monitoring of $\mathrm{cut}_{q_\mathrm{T}/q}$ and for extrapolation $\mathrm{cut}_{q_\mathrm{T}/q} \to 0$.

External ingredients: amplitudes applied in the calculation

1-loop amplitudes with OPENLOOPS [Cascioli, Maierhöfer, Pozzorini (2011); Cascioli, Lindert, Maierhöfer, Pozzorini (2014)]

- All tree and (squared) one-loop amplitudes (including colour/helicity correlations)
- Fully automated compact and fast numerical code for any SM process (QCD+EW)
- **Tensor reduction by means of the COLLIER library** [Denner, Dittmaier, Hofer (2014)]
  - Numerically stable Denner–Dittmaier reduction methods [Denner, Dittmaier (2002 & 2005)]
  - Scalar integrals with complex masses [Denner, Dittmaier (2010)]
- **Rescue system based on quad-precision CUTTOOLS** [Ossola, Papadopoulos, Pittau (2008)]
  - Scalar integrals from ONELOOP [van Hameren, Papadopoulos, Pittau (2009); van Hameren (2010)]

2-loop amplitudes from analytic results

- Drell–Yan-like amplitudes from [Matsuura, van der Marck, van Neerven (1989)]
- $V\gamma$ helicity amplitudes from [Gehrmann, Tancredi (2011)] , using TDHPL [Gehrmann, Remiddi (2001)]
- On-shell VV amplitudes from private code [von Manteuffel, Tancredi (2014)] , using GINAC (applied in [Cascioli et al. (2014); Gehrmann et al. (2014); Grazzini, SK, Rathlev, Wiesemann (2015)])
- Off-shell helicity VV' amplitudes from VVAMP [Gehrmann, von Manteuffel, Tancredi (2015)] , using GINAC [Bauer, Frink, Kreckel (2002); Vollinga, Weinzierl (2005)]
  (independent calculation by [Caola, Henn, Melnikov, Smirnov, Smirnov (2014)])

Numerical stability and dependence on $\mathrm{cut}_{q_T/q}$ in $\mathrm{pp} \to \mathrm{W}^+\mathrm{W}^- + X$

$\mathbf{q_T}$ subtraction at NLO

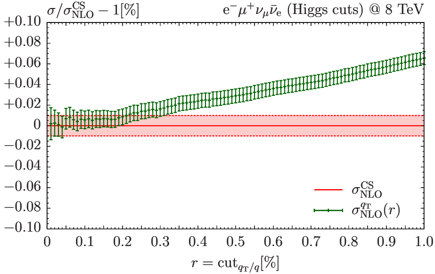

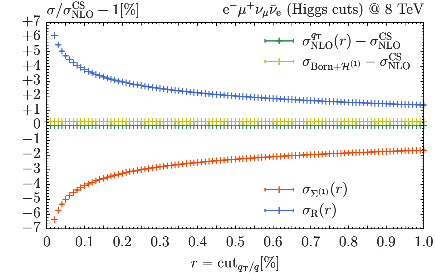

$\mathbf{q_T}$ subtraction at NNLO

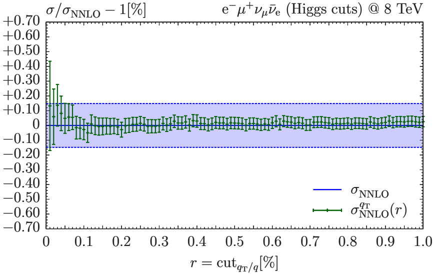

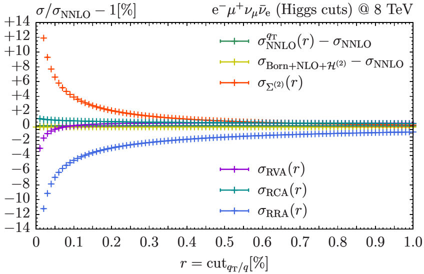

On-shell WW cross section and p_T-veto efficiencies with resummation

Relevant for extrapolation from fiducial to inclusive cross section:

p_T-veto efficiency

$$\epsilon(p_T^{\mathrm{veto}}) = \sigma(p_T < p_T^{\mathrm{veto}})/\sigma_{\mathrm{tot}} \, .$$

The p_T-veto efficiency considered here refers to the transverse momentum of the WW system; it is not the jet-veto efficiency.

However, the two transverse momenta are clearly correlated (and coincide up to $\mathcal{O}(\alpha_s)$).

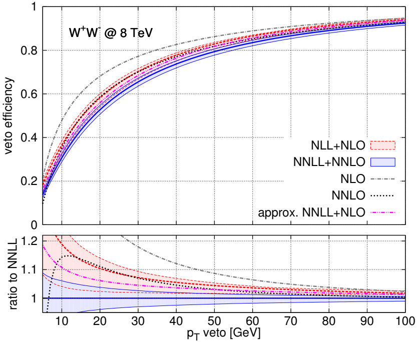

Latest CMS measurement applies approx. NNLL+NLO prediction in the extrapolation:

- CMS WW measurement [CMS collaboration (2015)] : good agreement with NNLO prediction

$$\sigma_{\mathrm{CMS}} = 60.1 \pm 0.9(\mathrm{stat}) \pm 3.2(\mathrm{exp}) \pm 3.1(\mathrm{th}) \pm 1.6(\mathrm{lumi})$$
$$\sigma_{\mathrm{NNLO}} = 59.84^{+1.3}_{-1.1}(\mathrm{scale}) \pm 1.2(\mathrm{pdf}) \qquad (\text{no Higgs contribution included})$$

- ATLAS WW measurement [ATLAS collaboration (2016)] : slight excess of $\approx +1.4\sigma$ wrt. NNLO

$$\sigma_{\mathrm{ATLAS}} = 71.1 \pm 1.1(\mathrm{stat})^{+5.7}_{-5.0}(\mathrm{syst}) \pm 1.4(\mathrm{lumi})$$
$$\sigma_{\mathrm{NNLO}} = 63.2^{+1.6}_{-1.2}(\mathrm{scale}) \pm 1.2(\mathrm{pdf}) \qquad (\text{Higgs contribution included})$$

Definition of WW signal/Higgs background cuts

cut variable	WW cuts	Higgs cuts
lepton definition		
p_{T,ℓ_1}	> 25 GeV	> 22 GeV
p_{T,ℓ_2}	> 20 GeV	> 10 GeV
$\lvert y_\mu \rvert$	< 2.4	< 2.4
$\lvert y_e \rvert$	< 2.47 and $\notin [1.37; 1.52]$	< 2.47 and $\notin [1.37; 1.52]$
leptonic cuts		
$p_{\mathrm{T,miss}}$	> 20 GeV	> 20 GeV
$p_{\mathrm{T,miss}}^{\mathrm{rel}}$	> 15 GeV	—
$p_{\mathrm{T},\ell\ell}$	—	> 30 GeV
$m_{\ell\ell}$	> 10 GeV	$\in [10\,\mathrm{GeV}; 55\,\mathrm{GeV}]$
$\Delta R_{\ell\ell}$	> 0.1	—
$\Delta\phi_{\ell\ell}$	—	< 1.8
$\Delta\phi_{\ell\ell,\nu\nu}$	—	$> \pi/2$
anti-k_{T} jets with $R = 0.4$, $p_{\mathrm{T},j} > 25$ GeV, $\lvert y_j \rvert < 4.5$		
N_{jets}	0	0

Distributions at 13 TeV with WW signal cuts: m_T^{ATLAS}, $p_{T,ll}$

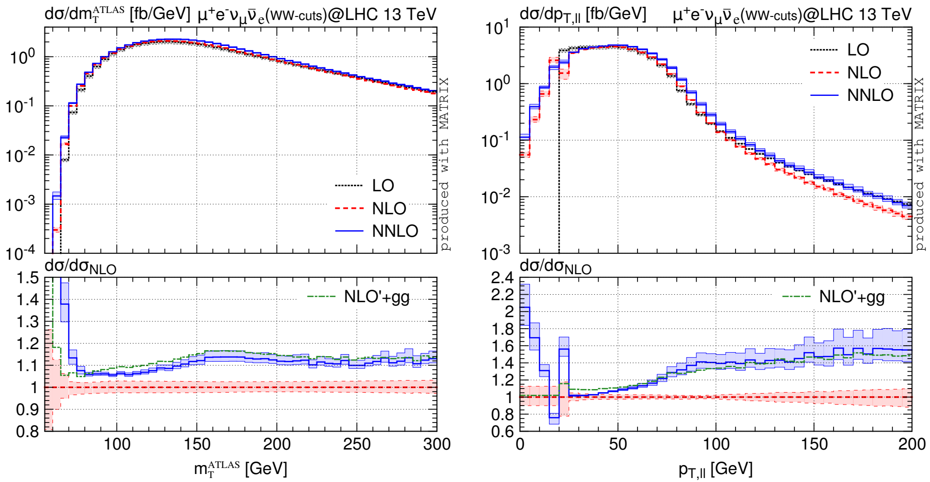

Distributions at 13 TeV with Higgs background cuts: p_{T,l_1}, p_{T,l_2}

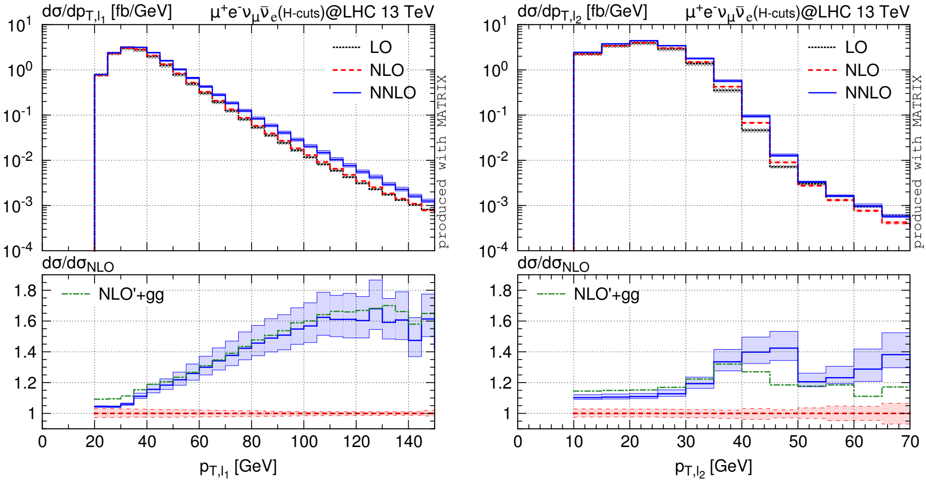

Distributions at 13 TeV with Higgs background cuts: $p_{T,\mathrm{miss}}$, $p_{T,ll}$

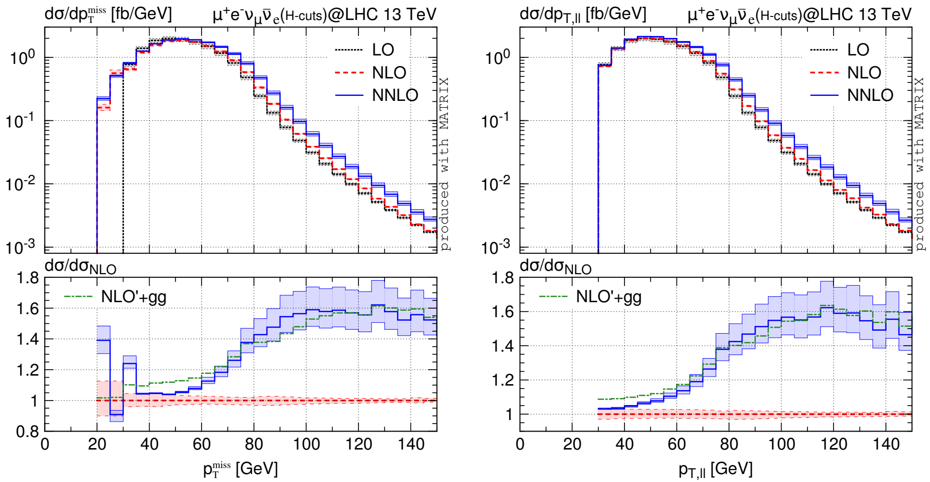

Distributions at 13 TeV with Higgs background cuts: m_{ll}, m_T^{ATLAS}

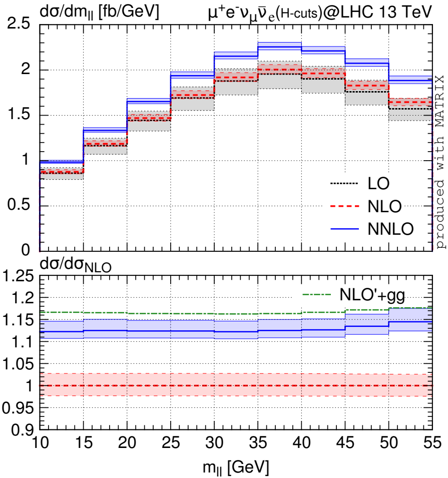

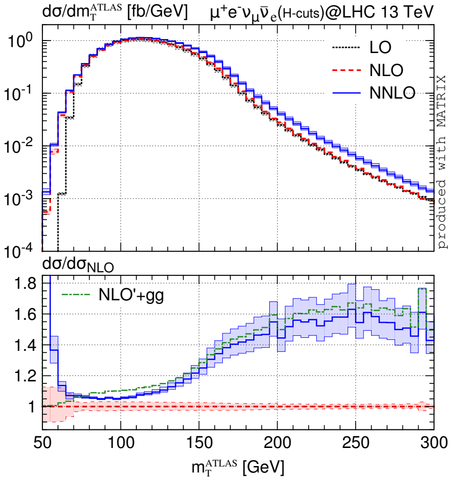

Distributions at 13 TeV with Higgs background cuts: $\Delta\phi_{ll}$, $\Delta\phi_{ll,\nu\nu}$